How frequent are Antarctic sudden stratospheric warmings in present and future climate?

M. Jucker[1,2], T. Reichler[3], and D. W. Waugh[4,5]

[1]Climate Change Research Centre, The University of New South Wales, Sydney, NSW, Australia
[2]Australian Research Council Centre of Excellence for Climate Extremes, Sydney, NSW, Australia
[3]Department of Atmospheric Sciences, University of Utah, Salt Lake City, UT, USA
[4]Department of Earth and Planetary Sciences, The Johns Hopkins University, Baltimore, MD, USA
[5]School of Mathematics and Statistics, The University of New South Wales, Sydney, NSW, Australia

Key Points:

- Antarctic sudden stratospheric warmings occur once every 22 years in present-day (1990) climate conditions.
- The warmings will become much rarer under future climate change, irrespective of their exact definition.
- The future decrease in frequency is linked to a strengthening of the Antarctic polar vortex.

Corresponding author: Martin Jucker, `publications@martinjucker.com`

Abstract

Southern Hemisphere (SH) Stratospheric Sudden Warmings (SSWs) result in smaller Antarctic ozone holes and are linked to extreme midlatitude weather on subseasonal to seasonal timescales. Therefore, it is of interest how often such events occur and whether we should expect more events in the future. Here, we use a pair of novel multi-millennial simulations with a stratosphere-resolving coupled ocean-atmosphere climate model to show that the frequency of SSWs, such as observed 2002 and 2019, is about one in 22 years for 1990 conditions. In addition, we show that we should expect the frequency of SSWs–and that of more moderate vortex weakening events–to strongly decrease by the end of this century.

Plain Language Summary

The stratosphere at 10-50 km height can influence surface weather for several months. In 2002 and 2019, the stratosphere warmed over Antarctica within a few days to weeks. This caused dry and hot summers in Australia and South America. And it reduced the size of the ozone hole. Since these warming events are rare, it is difficult to say how often they occur. We therefore use long computer simulations to answer that question. We find that without climate change, warming events occur about every 22 years. But with climate change, the warming events will happen only once every 300 years. From this, we believe that the quick succession of two events in 2002 and 2019 will remain special in history.

1 Introduction

The stratospheric polar vortex forms in the winter hemisphere due to the lack of solar heating at high latitudes and the resulting strong equator-to-pole temperature gradient. In the Northern Hemisphere (NH), strong and planetary scale waves originating in the troposphere from orographic forcing and land-sea contrast periodically propagate upward into the stratosphere and perturb the polar vortex via momentum deposition when the waves break (Eliassen & Palm, 1960; Charney & Drazin, 1961; Matsuno, 1971). In extreme cases, this disruption of the polar vortex leads to a rapid warming and reversal of wind directions in the polar stratosphere, a so-called (major) Sudden Stratospheric Warming (SSW) (Butler et al., 2015). These SSWs occur around every other winter in the NH.

However, over the six decades that we have station records (and later satellite observations) of the Southern Hemisphere (SH) polar vortex, only one such wind reversal has been recorded in 2002 (Roscoe et al., 2005). This event substantially decreased the size of the ozone hole thanks to higher than usual stratospheric polar temperatures and transport of ozone-rich air from lower latitudes into the polar regions (Fig. S1a) (Stolarski et al., 2005). There was also a dynamical effect of the 2002 SSW at the surface, as an extreme negative polarity of the Southern Annular Mode (SAM) was recorded at the surface for the 10-90 day period following the event (Thompson et al., 2005). Even though no wind reversal at 60° S and 10 hPa was registered in 2019, the polar vortex in this more recent event weakened dramatically and also lead to a smaller ozone hole (Fig. S1b) with almost 30% higher total column ozone values compared to the previous decade (Safieddine et al., 2020). The event has also been linked to the severe bushfire season in South Eastern Australia the following spring and summer (SPARC, 2020).

Due to the impacts on stratospheric ozone and surface weather on the subseasonal to seasonal timescale, it is important to determine how rare SSWs are in the SH, and whether we should expect more or less frequent SSWs under future climate change. However, given the shortness of the observational record it is impossible to get an observational estimate of how often SSWs do occur on average. Recently, Wang et al. (2020)

analyzed hindcasts of a seasonal forecasting system and found an average Antarctic SSW frequency of one every 25 years. However, the underlying model of this study had a strong mean westerly wind bias, raising some doubts on the validity of their results. Here, we revisit the question of how frequent Antarctic SSWs are in present climate and also address possible changes under future climate change. This is accomplished by investigating two nearly 10,000-year long simulations with a well-performing stratosphere-resolving coupled ocean-atmosphere model based on present-day (1990) and future (increased CO2) conditions and by considering integrations from the sixth Climate Model Intercomparison Project (CMIP6).

2 Model data and SSW definitions

2.1 Multi-millennial coupled GCM simulations

We use a set of two 9,900-year long simulations with the stratosphere-resolving version of the the Geophysical Fluid Dynamics Laboratory's CM2.1 atmosphere-ocean coupled climate model (Delworth et al., 2006; Horan & Reichler, 2017), which has been used in particular for studies of stratosphere-troposphere coupling in the past (Horan & Reichler, 2017; Jucker & Reichler, 2018). The model has 48 vertical levels with approximately half of the levels situated in the stratosphere and a model top at 0.002 hPa. The horizontal resolution is approximately 2° in latitude and 2.5° in longitude. The boundary conditions are set to perpetual 1990 conditions. More specifically, ozone in the year 1990 is comparable to both 2002 and the 2010s (Newman & Nash, 2019). The two simulations differ in their greenhouse gas forcing; CO_2 is set to 353 ppm in the 'present-day' and 1120 ppm in the 'future' simulation, which is a quadrupling relative to pre-industrial CO_2 concentration (and 3.2 times present-day concentration). This is the only difference between the two simulations. Atmospheric variables are stored on a daily frequency to allow for detailed dynamical analysis, including Eliassen-Palm fluxes.

In agreement with Reichler and Kim (2008) and Horan and Reichler (2017) who have shown that this model compares well to reanalysis in the troposphere and northern hemisphere stratosphere, both the southern hemisphere stratospheric zonal mean zonal wind and vertical component of the Eliassen-Palm flux from our present-day simulation show excellent agreement with those from ERA5 reanalysis (1979-2019) (Hersbach et al., 2020), for both mean and standard deviation (Fig. 1a,c). Besides its performance in the stratosphere which is of particular relevance here, the oceanic component has been validated extensively and also found to have a good representation of tropical (including ENSO, Wittenberg et al., 2006) as well as extratropical southern hemisphere ocean dynamics (Gnanadesikan et al., 2006).

Having multi-millennial simulations with a model showing such small bias will allow us to robustly estimate SSW frequencies. In addition, having future projections will make it possible to address the question of whether or not we should expect another SSW to occur, which we will show to be impossible without information on the impact of increased greenhouse gas concentrations.

2.2 SSW definitions

We follow the most common definition of Sudden Stratospheric Warmings as the reversal of u_{1060}, the zonal mean zonal wind at 60°S and 10 hPa ('SSW-reversal', Charlton & Polvani, 2007). However in observations, only the September 2002 event is a SSW-reversal event, while the 2019 event is widely considered a SSW but did not show wind reversal at 60°S and 10 hPa. Therefore, we have performed our analysis with an additional definition, allowing for a more general determination of SSW frequency and future change.

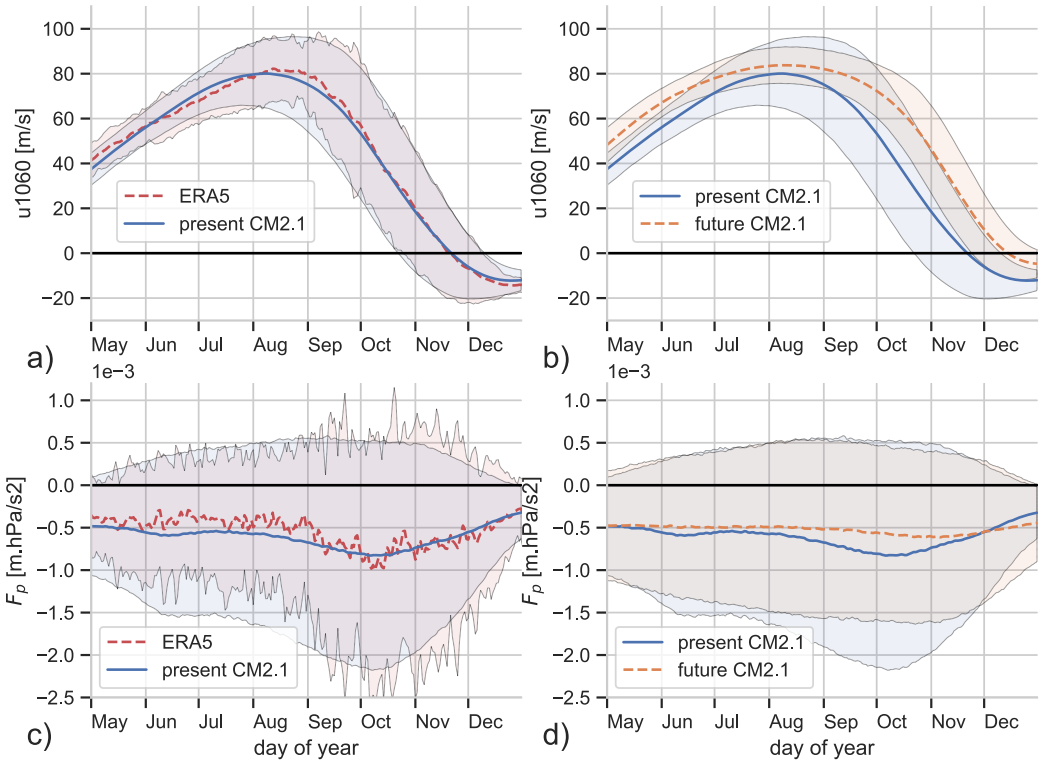

Figure 1. (top) Climatological mean (solid) and 2σ variability (shaded) of zonal mean zonal wind at 60°S and 10 hPa (u_{1060}) for (a) present-day CM2.1 and ERA5 and (b) present-day and future CM2.1. (bottom) same but for vertical EP flux. The present-day simulation (blue, solid) reproduces both mean and variability of the ERA5 reanalysis (1979-2019; red, dashed) in both u_{1060} (a) and vertical EP flux (c). The future simulation (orange, dashed) shows a clear strengthening of the polar vortex throughout the year (b) and a weakening of the vertical EP flux (d), in particular during the spring.

We found that the simplest method to define SSWs in the SH which detects both 2002 and 2019 as the only events during the satellite era is that the zonal mean zonal wind anomaly with respect to the day of the year at 60°S and 10 hPa passes below -40 m/s. The onset date is then defined as the day when the zonal mean zonal wind anomaly crosses -20 m/s for the last time before crossing -40 m/s. These 'SSW-weak' events follow the common features of stratosphere-troposphere coupling in the SH in their significant surface impact on monthly timescales (Fig. S2).

For both definitions, two events have to be separated by at least 20 days, and the onset date has to be at least 20 days before the vortex breakdown, which is defined as the last day of the year when u_{1060} becomes negative.

Finally, we follow Lim et al. (2018) who showed that weaker events can also have an impact at the surface, and we will also report results from their detection method based on the yearly timeseries of the first Principal Component of de-seasonalized monthly mean zonal mean zonal wind between 55 and 65°S. The corresponding Empirical Orthogonal Function is two-dimensional but in month of the year–pressure space (instead of the conventional longitude–latitude space) and is centered around the vortex breakdown in spring (the 'L18' method). This method does not provide onset dates, as there is only one value per year, and L18 is closely related to variations in the date of the vortex breakdown (positive for earlier breakdown; the correlation coefficient between the first Principal Component and the vortex breakdown date is $r = 0.79$ in ERA5 data, not shown). Following Lim et al. (2019), we apply a threshold of 0.8 standard deviations, which detects many more events than the other two definitions.

3 Occurrence of SSWs in the Southern Hemisphere

The present-day 9,900-year simulation produces 458 SSW-weak and 159 SSW-reversal events, corresponding to an average frequency of about one SSW-weak every 22 years and one SSW-reversal every 59 years. This compares well with the single SSW-reversal and only two SSW-weak events in the 42-year long satellite observation record (and the 63-year long non-satellite observational record since 1957 (Roscoe et al., 2005; Naujokat & Roscoe, 2005)), as well as Wang et al. (2020). In addition to yearly occurrence, we also analyze the seasonal occurrence of SSWs and find that the SSW-weak criterion detects events during the entire winter, with a peak occurrence in late August to September (Fig. 2d) and a mean occurrence of 27 August (note that early events in June and July have a similar impact as later events, not shown). The 2002 SSW occurred in late September, a time of the year when we estimate the mean return time of SSW-weak events to be 113 years, and the 2019 SSW occurred in early September, when the mean return time is estimated to be 102 years (Fig. 2a). Irrespective of time of the year, our present-day simulations indicate that we should expect between 0 and 6 SSW-reversals and between 0 and 12 SSW-weak events per century, with most likely numbers of 0-2 SSW-reversal and 3-6 SSW-weak events per century (25^{th} and 75^{th} percentiles, Figs. 2b,e). As indicated before, L18 events are much more abundant, with an occurrence of 7-36 events per century and a mean return time of one in 5 years (Fig. 2h).

To get an estimate of when the next SSW might occur, we perform a return time analysis where we produce a histogram of the number of SSWs which occur within a given time interval (Fig. 2c,f,i). If SSWs are independent and random events, we can compare the observed return time distribution to a theoretical distribution (S.5). The return time histogram follows closely the theoretical distribution for all methods, suggesting that in the SH, SSWs are independent and random, with a mean return time of about 59 years for SSW-reversal and 22 years for SSW-weak, or an annual probability of occurrence of 1.6% for SSW-reversal and 4.6% for SSW-weak. Using the theoretical survival function, we can then compute the probabilities of various scenarios (reported in Table 1). All of these probabilities are consistent with the observational record of one SSW-reversal and

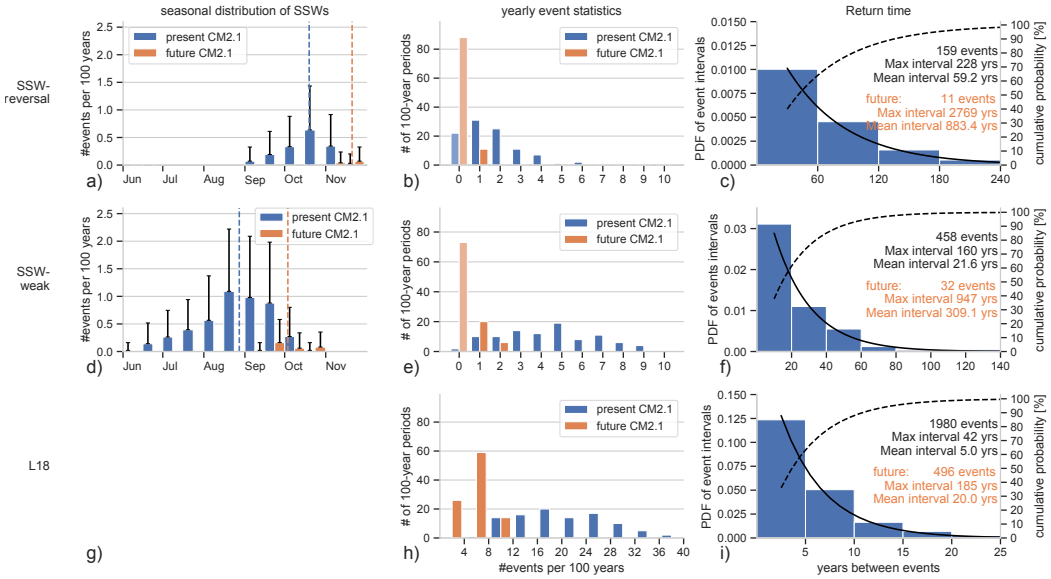

Figure 2. Event statistics: (left) Seasonal distribution, (middle) histogram of number of events per century, and (right) return time distribution histograms (bars) and theoretical distribution (black lines) for probability (solid) and cumulative distribution functions (dashed). Statistics are shown for (top) SSW-reversal, (middle) SSW-weak and (bottom) L18. For all plots, the present-day simulation is in blue and increased CO_2 ('future') in orange. On the left panels, statistics are shown for half-monthly intervals, the black whiskers show the standard deviation, and the vertical dashed lines indicate the mean date of occurrence. Panel (g) is empty as there is no seasonal information for L18. Note the differences in scales between rows. In panels (b) and (e), bars are drawn for each year, whereas in panel (h), the bars are drawn within intervals designated by the tick marks. Bars showing the number of centuries without event are pale.

		SSW-weak	SSW-reversal
present	Yearly probability	4.6%	1.6%
	Probability of less than observation	43%	52%
	Probability of exact observation	28%	35%
	Probability of more than observation	30%	15%
	Probability > 50% after	15 years	41 years
future	Yearly probability	0.3%	0.1%
	Probability > 50% after	214 years	612 years
	Probability of at least one SSW in 80 years	23%	8.7%
	Probability of at least two SSWs in 80 years	2.8%	0.4%

Table 1. Results from the theoretical fitting of the return times (Figs. 2c and f). Yearly probability is the probability of an event occurring during any given year (1/mean return time), probability of exact observation is computed for 2 SSW-weak and 1 SSW-reversal in 41 years. Time periods give the interval after which an SSW is more probable than not (probability of one or more events > 50%). The labels 'present' and 'future' refer to the relevant CM2.1 simulations, and we use an 80-year period to represent the time span 2021-2100 in the future simulation. Note that the observation percentages in the present simulation add to 101 instead of 100 due to rounding errors.

two SSW-weak events during the satellite era. Finally, neglecting any changes in climate from further greenhouse gas forcing since 1990, we estimate from the present-day simulation that the probability of at least one SSW by the end of the century (next 80 years) would be 74% for SSW-reversals and 98% for SSW-weak events. Of course, this is only hypothetical as greenhouse gas concentrations have already risen since 1990 and are projected to further increase in the future.

4 Enhanced greenhouse gas forcing

To estimate the impact of enhanced greenhouse gas forcing on the occurrence of SSWs in the SH, we conducted a second 9,900 year long simulation using increased CO_2 corresponding to the end of the century (1120 ppm instead of 353 ppm, henceforth called 'future'). The occurrence of SSWs in this simulation decreases drastically. The number of SSW-reversals reduces from 159 SSWs for present-day to only 11 in the future simulation, while SSW-weak events decrease from 458 to only 32 (Fig. 2). This translates into a return time of one SSW-reversal every 883 and one SSW-weak every 309 years, and a maximum of 1 SSW-reversal and 2 SSW-weak events per century. Note how the most probable outcome by far for any given 100-year period is zero SSWs (median is zero for both SSW-reversal and SSW-weak; Fig. 2b and e, orange). From the theoretical fit, the probability of occurrence of at least one SSW-weak event in 80 years is now about 23% (2.8% for at least two SSWs; Table 1). The analysis also suggests that SSW-reversals become very rare (probability of 8.7% within 80 years). SSWs not only become much rarer, but are also occurring later in the year, with a mean date of 3 October for SSW-weak, i.e. more than one month later than in the present-day simulation. For all definitions, there is a strong tendency for fewer SSWs in the future–including L18, which reduce to 0-11 events per century. Thus, while the 2019 event is consistent with the occurrence rate in our present-day simulation, it is inconsistent with the rate seen in our future simulation. Given the trend in SSW frequency, and that we are already one-third of the way towards the year 2080, we conclude that this latest event should not be attributed to increased CO_2 forcing, and might indeed be the last observed event this century.

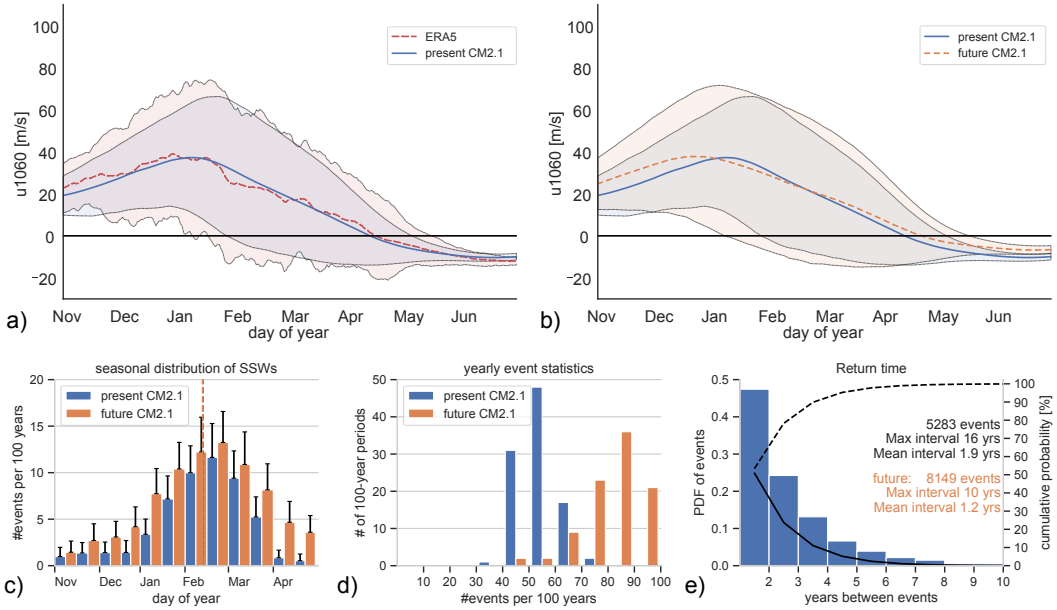

Figure 3. (top) u_{1060} for the Northern Hemisphere (NH) for (a) present-day and (b) increased CO_2 ('future'), similar to Fig. 1. (bottom) NH SSW-reversal statistics for (c) seasonal distribution, (d) number of events per century and (e) return time, similar to Fig. 2. Note the differences in scale of the bottom row compared to Fig. 2, which is a result of the higher occurrence rate for the NH.

The decrease in SSW frequency in the future is accompanied by a strengthening of the SH polar vortex (Fig. 1b), which can be linked to stronger radiative cooling under increased greenhouse gas concentrations (Thompson et al., 2012; Santer et al., 2013). In addition, our simulations suggest a decrease in wave forcing, more so during spring than other times of the year (Fig. 1d). Together with an earlier study, which found a direct link between the SSW-reversal frequency and polar vortex strength (Jucker et al., 2014), our results suggest that the projected strengthening of the polar vortex along with a decrease in wave forcing are responsible for a substantial decrease in the probability of occurrence of SSWs.

5 Comparison to NH

The occurrence of SSWs in the NH is very different from the SH, not just because of the much higher SSW frequency at present, but also in terms of future projections of both polar vortex strength and SSW frequency. As discussed in detail by Horan and Reichler (2017), our model climatology and variability in the NH compares well to reanalysis products (Fig. 3), and it produces about five SSWs per decade in the NH, in accordance with observations (Jucker & Reichler, 2018). Therefore, we perform the same analysis for the NH and briefly report our findings here.

The return time distribution shows that at intervals shorter than four years, NH SSWs are not independent and random (Fig. 3e), probably reflecting the influence of slowly evolving large scale climate modes, such as the El Niño Southern Oscillation or the Quasi-Biennial Oscillation, on the occurrence of SSWs (Holton & Tan, 1980; Taguchi & Hartmann, 2006; Anstey & Shepherd, 2014). The NH polar vortex is also weaker and more influenced by upward propagating planetary waves from the troposphere, resulting in a

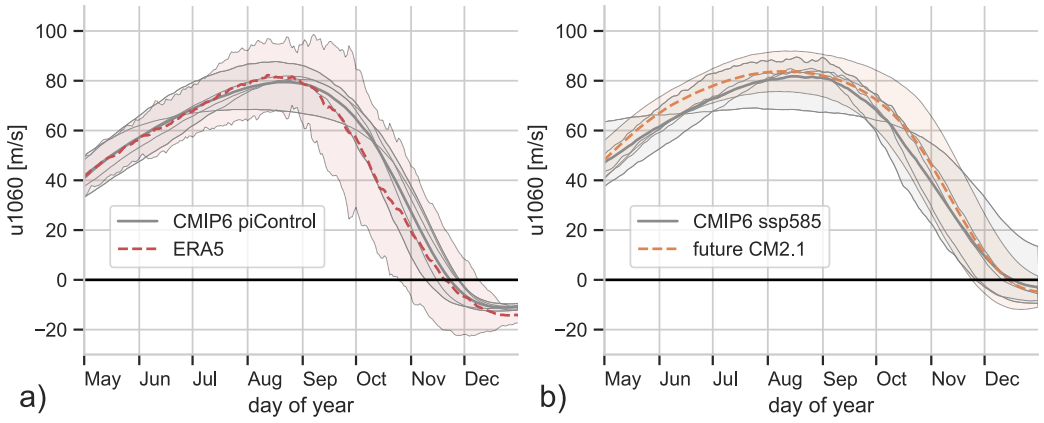

Figure 4. Analysis similar to Fig. 1, but using CMIP6 data. SSP585 data represents the climatology over 2080-2100. Shading corresponds to the range of model means (min to max), whereas the thin solid gray lines show each model and the thick gray and purple lines the multi model means.

more variable polar vortex than in the SH (Fig. 3, top). Our simulations suggest a slightly weaker polar vortex and more SSWs in the future NH (Fig. 3, bottom; SSW-reversal only). However, we have less confidence in this result because strong dynamical coupling between the troposphere and the stratosphere in the NH complicates future projections, and also because several past studies were unable to reach a consensus on possible future changes of SSW occurrence rates over the NH (Manzini et al., 2014; Ayarzagüena et al., 2018; Wu et al., 2019; Ayarzagüena et al., 2020). Coincidentally, there is also no consensus about the future strength of the polar vortex (Simpson et al., 2018), which is in agreement with our conclusion that the polar vortex strength is important for the frequency of SSWs.

6 CMIP6

To check the robustness of our single model simulations, we repeat our analysis with CMIP6 data (see Sec. S.3 for details). We find that these models show a positive polar vortex strength bias (Fig. 4) and generally struggle to produce the observed frequency of SSWs, with a range of 0.3-2.4 SSW-weak events on average in 80 years for piControl (Table S1). The low SSW frequency in CMIP6 was also briefly noted in recent work (Ayarzagüena et al., 2020). However, the statistical analysis again suggests a decrease in SSWs in the future, with three models producing one single and two models producing no SSW-weak event in SSP585 between 2021 and 2100 (Table S1b). The CMIP6 models consistently project a strengthening of the SH polar vortex of similar amplitude as our simulations with CM2.1 (Fig. 4), suggesting that our main conclusion that SSWs will become much rarer in the future is robust.

Our enhanced CO_2 CM2.1 simulation only considers future increases in CO_2. Changes in other radiatively active gases, in particular the expected recovery of the ozone hole by 2080 (Dhomse et al., 2018), are not included. However, our 1120 ppm CO_2 concentration is equal to the CO_2 concentration at the end of the century following the SSP585 scenario (which in addition to CO_2 also increases other greenhouse gases such as methane and nitrous oxide (O'Neill et al., 2016; Meinshausen & Nicholls, 2020)). Consequently, u_{1060} of our future simulation compares well to the end of the 21st century in CMIP6 SSP585 model data (Fig. 4b). This is consistent with previous findings that over the long

term, the greenhouse effect from increasing CO_2 concentrations dominates the effect of the ozone hole recovery (Barnes & Polvani, 2013). The similarities in u_{1060} and CO_2 concentrations between our CM2.1 simulations and CMIP6 models gives us confidence that our enhanced CO_2 simulation is relevant for end-of-century projections.

7 Conclusions

The 2002 and 2019 SSWs both resulted in exceptionally small ozone holes as have not been observed since the 1980s. They were also followed by extended periods of negative Southern Annular Mode at the surface, and 2019 in particular was linked to the catastrophic fire season in South Eastern Australia. While possibly predictable on the seasonal time scale, it has been difficult to determine how often SSWs should be expected in the southern hemisphere, due to a relatively short observational record on one hand and large model biases in the southern hemisphere stratosphere in most comprehensive climate models on the other hand. Using a pair of exceptionally long and low bias climate model runs, we found that while SSWs in the SH have significant impacts on stratospheric ozone and surface weather, such events are rare and will become even rarer as CO_2 concentrations increase. In our simulation based on 1990 conditions, the mean return time for events similar to the 2002 and 2019 SSWs is about 22 years, with a 57% chance of at least two and a 30% chance of three or more SSW-weak events happening within the time period spanned by the satellite record. Thus, it is no surprise that two events have been observed, and there would be a fair chance of another SSW (of either flavor) in the near future if CO_2 levels were kept constant. However, we show that one should not make predictions of future occurrence from past data; given that the world follows a high emissions pathway, our projections suggest that events similar to 2002 and 2019 will become extremely rare, with a mean return time of one in 309 years (or 0.3% each year) by the end of the century.

Acknowledgments

M.J. was supported by the Australian Research Council grant ARC grant FL150100035 and the ARC Centre of Excellence for Climate Extremes which is supported by the Australian Research Council via grant CE170100023. T. R. acknowledges support from NSF grant 1446292. We also acknowledge the Center for High Performance Computing at the University of Utah and the National Computational Infrastructure in Canberra for providing compute infrastructure and computing time. This work used the xarray (Hoyer & Hamman, 2017) and aostools (Jucker, 0) packages. The zonal mean zonal wind timeseries from our simulations are available at `https://data.mendeley.com/datasets/hknv82tz7v/draft?a=84a23625-6306-440f-ae69-19011c620c7a`. All authors contributed to conceptualization, methodology and writing of the original draft. T.R. provided the GCM simulations and M.J. performed the formal analysis. Authors declare no competing interests.

References

Anstey, J. A., & Shepherd, T. G. (2014, 1). High-latitude influence of the quasi-biennial oscillation. *Quarterly Journal of the Royal Meteorological Society*, *140*(678), 1–21. Retrieved from `http://doi.wiley.com/10.1002/qj.2132` doi: 10.1002/qj.2132

Ayarzagüena, B., Charlton-Perez, A. J., Butler, A. H., Hitchcock, P., Simpson, I. R., Polvani, L. M., ... Watanabe, S. (2020). Uncertainty in the Response of Sudden Stratospheric Warmings and Stratosphere-Troposphere Coupling to Quadrupled CO2 Concentrations in CMIP6 Models. *Journal of Geophysical Research: Atmospheres*, *125*(6), 1–21. doi: 10.1029/2019JD032345

Ayarzagüena, B., Polvani, L. M., Langematz, U., Akiyoshi, H., Bekki, S., Butchart,

N., ... Zeng, G. (2018, 8). No robust evidence of future changes in major stratospheric sudden warmings: a multi-model assessment from CCMI. *Atmospheric Chemistry and Physics*, *18*(15), 11277–11287. Retrieved from https://www.atmos-chem-phys.net/18/11277/2018/ doi: 10.5194/acp-18-11277-2018

Barnes, E. A., & Polvani, L. (2013, 9). Response of the Midlatitude Jets, and of Their Variability, to Increased Greenhouse Gases in the CMIP5 Models. *Journal of Climate*, *26*(18), 7117–7135. Retrieved from http://journals.ametsoc.org/doi/abs/10.1175/JCLI-D-12-00536.1 doi: 10.1175/JCLI-D-12-00536.1

Butler, A. H., Seidel, D. J., Hardiman, S. C., Butchart, N., Birner, T., & Match, A. (2015, 1). Defining sudden stratospheric warmings. *Bulletin of the American Meteorological Society*, *96*(2), 150904101253006. Retrieved from http://journals.ametsoc.org/doi/abs/10.1175/BAMS-D-13-00173.1 doi: 10.1175/BAMS-D-13-00173.1

Charlton, A. J., & Polvani, L. M. (2007, 2). A New Look at Stratospheric Sudden Warmings. Part I: Climatology and Modeling Benchmarks. *Journal of Climate*, *20*(3), 449–469. Retrieved from http://journals.ametsoc.org/doi/abs/10.1175/JCLI3996.1 doi: 10.1175/JCLI3996.1

Charlton-Perez, A. J., Baldwin, M. P., Birner, T., Black, R. X., Butler, A. H., Calvo, N., ... Watanabe, S. (2013). On the lack of stratospheric dynamical variability in low-top versions of the CMIP5 models. *Journal of Geophysical Research Atmospheres*, *118*(6), 2494–2505. doi: 10.1002/jgrd.50125

Charney, J., & Drazin, P. (1961). Propagation of Planetary-Scale Disturbances from the Lower into the Upper Atmosphere. *J. Geophys. Res*, *66*, 83–109. Retrieved from http://climateknowledge.org/figures/Rood_Climate_Change_AOSS480_Documents/QC109_Charney_Drazin_Propagation_Planetary_Waves_JGR_1961.pdf

Delworth, T. L., Broccoli, A. J., Rosati, A., Stouffer, R. J., Balaji, V., Beesley, J. a., ... Zhang, R. (2006, 3). GFDL's CM2 Global Coupled Climate Models. Part I: Formulation and Simulation Characteristics. *Journal of Climate*, *19*(5), 643–674. Retrieved from http://journals.ametsoc.org/doi/abs/10.1175/JCLI3629.1 doi: 10.1175/JCLI3629.1

Dhomse, S. S., Kinnison, D., Chipperfield, M. P., Salawitch, R. J., Cionni, I., Hegglin, M. I., ... Zeng, G. (2018). Estimates of ozone return dates from Chemistry-Climate Model Initiative simulations. *Atmospheric Chemistry and Physics*, *18*(11), 8409–8438. doi: 10.5194/acp-18-8409-2018

Eliassen, A., & Palm, T. (1960). On the transfer of energy in stationary mountain waves. *Geofys. Publ.*, *22*(3), 1–23.

Gillett, N. P., Kell, T. D., & Jones, P. D. (2006). Regional climate impacts of the Southern Annular Mode. *Geophysical Research Letters*, *33*(23), 1–4. doi: 10.1029/2006GL027721

Gnanadesikan, A., Dixon, K. W., Griffies, S. M., Balaji, V., Barreiro, M., Beesley, J. A., ... Dunne, J. P. (2006, 3). GFDL's CM2 Global Coupled Climate Models. Part II: The Baseline Ocean Simulation. *Journal of Climate*, *19*(5), 675–697. Retrieved from http://journals.ametsoc.org/doi/abs/10.1175/JCLI3630.1 doi: 10.1175/JCLI3630.1

Hersbach, H., Bell, B., Berrisford, P., Hirahara, S., Horányi, A., Muñoz-Sabater, J., ... Thépaut, J. (2020, 7). The ERA5 global reanalysis. *Quarterly Journal of the Royal Meteorological Society*, *146*(730), 1999–2049. Retrieved from https://onlinelibrary.wiley.com/doi/abs/10.1002/qj.3803 doi: 10.1002/qj.3803

Holton, J. R., & Tan, H.-C. (1980, 10). The Influence of the Equatorial Quasi-Biennial Oscillation on the Global Circulation at 50 mb. *Journal of the Atmospheric Sciences*, *37*(10), 2200–2208. Retrieved from http://

journals.ametsoc.org/doi/abs/10.1175/1520-0469%281980%29037%3C2200%3ATIOTEQ%3E2.0.CO%3B2 doi: 10.1175/1520-0469(1980)037⟨2200:TIOTEQ⟩2.0.CO;2

Horan, M. F., & Reichler, T. (2017, 12). Modeling Seasonal Sudden Stratospheric Warming Climatology Based on Polar Vortex Statistics. *Journal of Climate*, *30*(24), 10101–10116. Retrieved from http://journals.ametsoc.org/doi/10.1175/JCLI-D-17-0257.1 doi: 10.1175/JCLI-D-17-0257.1

Hoyer, S., & Hamman, J. J. (2017, 4). xarray: N-D labeled Arrays and Datasets in Python. *Journal of Open Research Software*, *5*, 1–6. Retrieved from http://openresearchsoftware.metajnl.com/articles/10.5334/jors.148/ doi: 10.5334/jors.148

Jucker, M. (0). *aostools - https://github.com/mjucker/aostools.* Zenodo. Retrieved from https://dx.doi.org/10.5281/zenodo.597598 doi: 10.5281/zenodo.597598

Jucker, M., Fueglistaler, S., & Vallis, G. K. (2014, 10). Stratospheric sudden warmings in an idealized GCM. *Journal of Geophysical Research: Atmospheres*, *119*(19), 054–11. Retrieved from http://doi.wiley.com/10.1002/2014JD022170 doi: 10.1002/2014JD022170

Jucker, M., & Reichler, T. (2018, 12). Dynamical Precursors for Statistical Prediction of Stratospheric Sudden Warming Events. *Geophysical Research Letters*, *45*(23), 124–13. Retrieved from http://doi.wiley.com/10.1029/2018GL080691https://onlinelibrary.wiley.com/doi/abs/10.1029/2018GL080691 doi: 10.1029/2018GL080691

Lewis, D. (2019, 10). Rare warming over Antarctica reveals power of stratospheric models. *Nature*, *574*(7777), 160–161. Retrieved from http://www.nature.com/articles/d41586-019-02985-8 doi: 10.1038/d41586-019-02985-8

Lim, E.-P., Hendon, H. H., Boschat, G., Hudson, D., Thompson, D. W. J., Dowdy, A. J., & Arblaster, J. M. (2019, 11). Australian hot and dry extremes induced by weakenings of the stratospheric polar vortex. *Nature Geoscience*, *12*(11), 896–901. Retrieved from http://dx.doi.org/10.1038/s41561-019-0456-xhttp://www.nature.com/articles/s41561-019-0456-x doi: 10.1038/s41561-019-0456-x

Lim, E.-P., Hendon, H. H., & Thompson, D. W. J. (2018, 11). Seasonal Evolution of Stratosphere-Troposphere Coupling in the Southern Hemisphere and Implications for the Predictability of Surface Climate. *Journal of Geophysical Research: Atmospheres*, *123*(21), 002–12. Retrieved from http://doi.wiley.com/10.1029/2018JD029321 doi: 10.1029/2018JD029321

Manzini, E., Karpechko, A. Y., Anstey, J., Baldwin, M. P., Black, R. X., Cagnazzo, C., ... Zappa, G. (2014, 7). Northern winter climate change: Assessment of uncertainty in CMIP5 projections related to stratosphere-troposphere coupling. *Journal of Geophysical Research: Atmospheres*, *119*(13), 7979–7998. Retrieved from http://doi.wiley.com/10.1002/2013JD021403 doi: 10.1002/2013JD021403

Matsuno, T. (1971, 11). A Dynamical Model of the Stratospheric Sudden Warming. *Journal of the Atmospheric Sciences*, *28*(8), 1479–1494. Retrieved from http://journals.ametsoc.org/doi/abs/10.1175/1520-0469(1971)028%3C1479:ADMOTS%3E2.0.CO;2 doi: 10.1175/1520-0469(1971)028⟨1479:ADMOTS⟩2.0.CO;2

Meinshausen, M., & Nicholls, Z. (2020). *Greenhouse Gas Factsheet, http://greenhousegases.science.unimelb.edu.au/.* Retrieved from http://greenhousegases.science.unimelb.edu.au/

Naujokat, B., & Roscoe, H. K. (2005). Evidence against an Antarctic stratospheric vortex split during the periods of pre-IGY temperature measurements. *Journal of the Atmospheric Sciences*, *62*(3), 885–889. doi: 10.1175/JAS-3317.1

Newman, P. A., & Nash, E. R. (2019). MERRA2. *NASA,*

ozonewatch.gsfc.nasa.gov.

O'Neill, B. C., Kriegler, E., Riahi, K., Ebi, K. L., Hallegatte, S., Carter, T. R., ... van Vuuren, D. P. (2014). A new scenario framework for climate change research: The concept of shared socioeconomic pathways. *Climatic Change*, *122*(3), 387–400. doi: 10.1007/s10584-013-0905-2

O'Neill, B. C., Tebaldi, C., Van Vuuren, D. P., Eyring, V., Friedlingstein, P., Hurtt, G., ... Sanderson, B. M. (2016). The Scenario Model Intercomparison Project (ScenarioMIP) for CMIP6. *Geoscientific Model Development*, *9*(9), 3461–3482. doi: 10.5194/gmd-9-3461-2016

Reichler, T., & Kim, J. (2008, 3). How Well Do Coupled Models Simulate Today's Climate? *Bulletin of the American Meteorological Society*, *89*(3), 303–312. Retrieved from `http://journals.ametsoc.org/doi/10.1175/BAMS-89-3-303` doi: 10.1175/BAMS-89-3-303

Roscoe, H. K., Shanklin, J. D., & Colwell, S. R. (2005). Has the Antarctic vortex split before 2002? *Journal of the Atmospheric Sciences*, *62*(3), 581–588. doi: 10.1175/JAS-3331.1

Safieddine, S., Bouillon, M., Paracho, A. C., Jumelet, J., Tencé, F., Pazmino, A., ... Clerbaux, C. (2020). Antarctic Ozone Enhancement During the 2019 Sudden Stratospheric Warming Event. *Geophysical Research Letters*, *47*(14), 1–10. doi: 10.1029/2020GL087810

Santer, B. D., Painter, J. F., Bonfils, C., Mears, C. A., Solomon, S., Wigley, T. M., ... Wentz, F. J. (2013). Human and natural influences on the changing thermal structure of the atmosphere. *Proceedings of the National Academy of Sciences of the United States of America*, *110*(43), 17235–17240. doi: 10.1073/pnas.1305332110

Simpson, I. R., Hitchcock, P., Seager, R., Wu, Y., & Callaghan, P. (2018). The downward influence of uncertainty in the Northern Hemisphere stratospheric polar vortex response to climate change. *Journal of Climate*, *31*(16), 6371–6391. doi: 10.1175/JCLI-D-18-0041.1

SPARC. (2020). Newsletter No 54. *http://www.sparc-climate.org/publications/newsletter/*, 10pp. Retrieved from `http://www.sparc-climate.org/publications/newsletter/`

Stolarski, R. S., McPeters, R. D., & Newman, P. A. (2005, 3). The Ozone Hole of 2002 as Measured by TOMS. *Journal of the Atmospheric Sciences*, *62*(3), 716–720. Retrieved from `https://journals.ametsoc.org/jas/article/62/3/716/25908/The-Ozone-Hole-of-2002-as-Measured-by-TOMS` doi: 10.1175/JAS-3338.1

Taguchi, M., & Hartmann, D. L. (2006, 2). Increased Occurrence of Stratospheric Sudden Warmings during El Niño as Simulated by WACCM. *Journal of Climate*, *19*(3), 324–332. Retrieved from `https://journals.ametsoc.org/jcli/article/19/3/324/31248/Increased-Occurrence-of-Stratospheric-Sudden` doi: 10.1175/JCLI3655.1

Thompson, D. W. J., Baldwin, M. P., & Solomon, S. (2005, 3). Stratosphere–Troposphere Coupling in the Southern Hemisphere. *Journal of the Atmospheric Sciences*, *62*(3), 708–715. Retrieved from `http://journals.ametsoc.org/doi/abs/10.1175/JAS-3321.1` doi: 10.1175/JAS-3321.1

Thompson, D. W. J., Seidel, D. J., Randel, W. J., Zou, C.-Z., Butler, A. H., Mears, C., ... Lin, R. (2012, 11). The mystery of recent stratospheric temperature trends. *Nature*, *491*(7426), 692–697. Retrieved from `http://www.nature.com/doifinder/10.1038/nature11579` doi: 10.1038/nature11579

Wang, L., Hardiman, S. C., Bett, P. E., Comer, R. E., Kent, C., & Scaife, A. A. (2020). What chance of a sudden stratospheric warming in the southern hemisphere? *Environmental Research Letters*, *15*(10). doi: 10.1088/1748-9326/aba8c1

Wittenberg, A. T., Rosati, A., Lau, N.-C., Ploshay, J. J., Wittenberg, A. T., Rosati,

A., ... Ploshay, J. J. (2006, 3). GFDL's CM2 Global Coupled Climate Models. Part III: Tropical Pacific Climate and ENSO. *Journal of Climate*, *19*(5), 698–722. Retrieved from `http://journals.ametsoc.org/doi/abs/10.1175/JCLI3631.1` doi: 10.1175/JCLI3631.1

Wu, Y., Simpson, I. R., & Seager, R. (2019). Intermodel Spread in the Northern Hemisphere Stratospheric Polar Vortex Response to Climate Change in the CMIP5 Models. *Geophysical Research Letters*, *46*(22), 13290–13298. doi: 10.1029/2019GL085545

Supplementary material

S.1 The 2002 and 2019 events

Fig. S1 shows the evolution of u_{1060} and polar cap stratospheric ozone during the springs of 2002 and 2019 from ERA5.

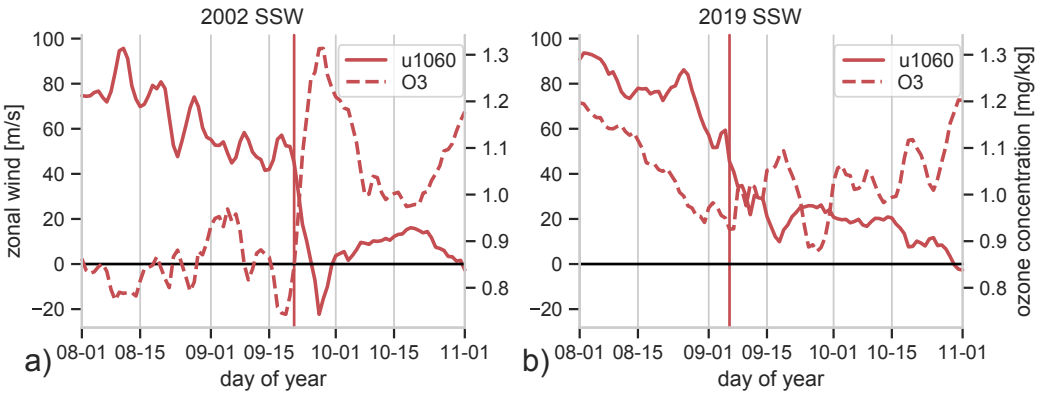

Figure S1. u_{1060} (solid), and polar cap (60-90°S) averaged ozone mass mixing ratio at 50 hPa (dashed) for the springs of (a) 2002 and (b) 2019 from ERA5 reanalysis. The solid vertical lines denote the onset date based on the SSW-weak definition.

S.2 Surface impacts

Just as for the observed SSWs, in our present-day simulation SSWs are followed by a negative phase of the SAM on a monthly to seasonal timescale (Fig. S2a; only composites for SSW-weak are shown) (Thompson et al., 2005), accompanied by colder and wetter conditions over New Zealand and South America as well as warmer and drier conditions over Eastern Australia (Figs. S2b and S2c). These surface impacts agree well with previous work (Gillett et al., 2006; Lewis, 2019; Lim et al., 2019) and the reanalysis data from the 2002 and 2019 events, confirming that our model reproduces the dynamical evolution of SSWs well and that our definition based on anomalous u_{1060} does indeed capture events with considerable surface impact. We note that the surface impact of early SSW-weak events (e.g. those occurring in June and July) is similar to the impact of later events (not shown).

S.3 CMIP6 model selection

We consider pre-industrial control (piControl) and Shared Socioeconomic Pathway 585 (SSP585) (O'Neill et al., 2014) simulations (which include e.g. ozone hole recovery, Fig. 4 and Table S1). The models from the CMIP6 archive were chosen based on the availability of daily data for both piControl and SSP585 scenarios, and given the lack of stratospheric variability in low top models (Charlton-Perez et al., 2013), we require a well resolved stratosphere with at least 30 vertical levels and a model top at or above 1 hPa. For piControl we required at least 100 years of data for sufficient statistics. The five models that fulfil all these conditions are CESM2-WACCM, CanESM5, GFDL-CM4, INM-CM5-0, MIROC6, and the data used comprise a total of 3,341 years of piControl as well as 5x80 years of SSP585 (from 2021 to 2100). One ensemble member (r1i1p1f) for each model was considered.

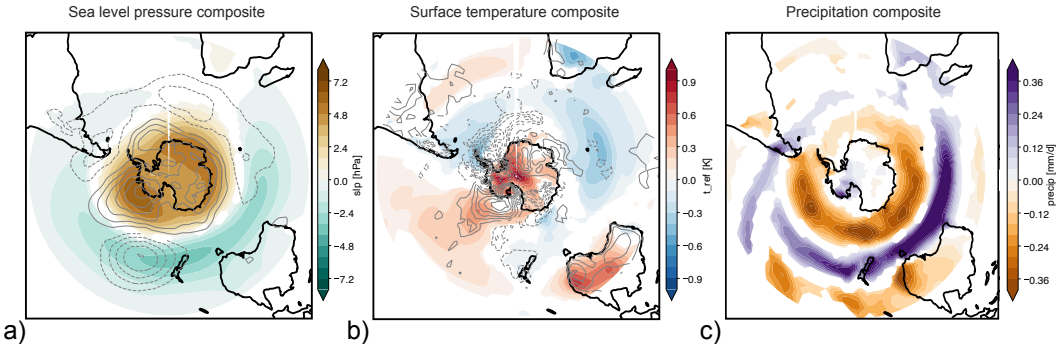

Figure S2. Composited surface anomalies averaged 0-60 days after the onset day for (a) surface pressure, (b) surface temperature and (c) precipitation for present-day CM2.1 SSW-weak events. The composites of the 2002 and 2019 events from ERA5 are added in gray contours for direct comparison except for precipitation which is too noisy in ERA5. Anomalies are relative to daily climatology, and only values which are statistically significant at the 5% level (t-test) are plotted.

Model	# years	# SSW-weak	mean return time [years]	# SSW-weak per 80 years	# SSW-weak 2021-2100
CESM2-WACCM	500	15	33.3	2.40	0
CanESM5	1000	6	166.7	0.48	1
GFDL-CM4	140	1	140.0	0.57	1
INM-CM5-0	1201	5	240.2	0.33	0
MIROC6	500	5	100.0	0.80	1

Table S1. Statistical information for CMIP6 data. All columns except the last refer to piControl simulations, whereas the last reports results from the SSP585 simulations. The second last column normalizes the number of SSW-weak events in piControl to a 80-year period for direct comparison to 2021-2100. All models except CESM2-WACCM strongly underestimate the number of SSWs, and no model produces more than one single event between 2021 and 2100.

S.4 Uncertainty estimates

For the two CM2.1 simulations, frequency uncertainties in Fig. 2 are computed by splitting the 9,900 years (after 90 years spinup) into 99 century-long non-overlapping segments, and computing the mean and standard deviation from this ensemble. For CMIP6 there are not enough events for similar statistical calculations, and the raw results are reported in Table S1.

S.5 Return time

If SSWs are random and independent, we should be able to model them as a Poisson process. For such a process, the return or waiting time can be computed using an exponential distribution with an expectation value equal to the mean occurrence frequency: PDF $= \lambda \exp(-\lambda x)$, where λ is the average frequency (e.g. 1/21.6 years for present-day SH SSW-weak events) and x is the waiting time in years. This is an approximation to a binomial distribution assuming large sample size and low probability. Since in our case we do not always have large sample size, we compute the return time using the binomial distribution. Then, the return time distribution is determined by the probability of zero events during a given time period ($k = 0$, n =number of years, $p = 1/$mean return time to be fitted). This has the advantage of being able to compute the probabilities for an arbitrary number of events, while still being able to check the validity of randomness and independence. The cumulative distribution function of the exponential distribution is an approximation (again large sample size and low probability) for the survival function of a binomial distribution for zero events. Therefore, we use the latter to compute the probability of one or more events within a given time period, provided the events are independent and random.

Explicitly, the return time PDF of a random and independent process follows a binomial distribution of zero events, as the return time corresponds to the probability of no event happening within a given time interval:

$$P(y) = \left[\sum_{k=0}^{k=N} \binom{y}{k} \left(\frac{1}{\tau}\right)^k \left(1 - \frac{1}{\tau}\right)^{y-k} \right]_{N=0} = \left(1 - \frac{1}{\tau}\right)^y, \tag{1}$$

where y is the time interval in years, $N(=0)$ is the number of events, and τ is the mean time interval between two SSWs (e.g. 21.6 years for present-day SSW-weak events). This is what is shown as solid black line in the return time plots of Fig. 2.

The probability of one or more events within a given time interval is simply $1 - P(y)$, which is shown as dashed black line in the return time plots. This so-called 'survival function' is used along with the cumulative probability function (as shown above but not setting $N = 0$) and the mass probability function (without the summation) to compute the various probabilities reported in the text and Table 1. For instance, the probability of at least one SSW-reversal in 80 years is $1 - (1 - 1/883)^{80} \approx 8.7\%$, and the probability of exactly two SSW-weak events in 41 years of present-day conditions is

$$\binom{41}{2} \left(\frac{1}{21.6}\right)^2 \left(1 - \frac{1}{21.6}\right)^{41-2} \approx 28\%, \tag{2}$$

as reported in Table 1.